

Supporting Information

Ultrathin Bilayer Membrane with Asymmetric Wettability for Pressure Responsive Oil/Water Emulsion Separation

*Liang Hu, Shoujian Gao, Yuzhang Zhu, Feng Zhang, Lei Jiang, and Jian Jin**

1. Photograph of a mixed cellulose ester (MCE) filter substrate supported bilayer membrane.

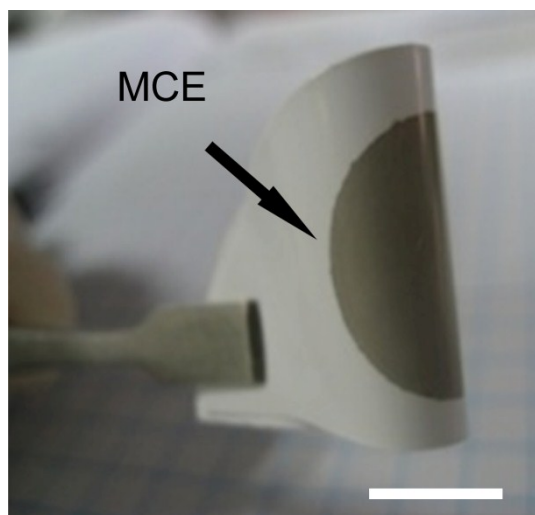


Figure S1. Photograph of a mixed cellulose ester filter substrate supported bilayer membrane. Scale bar = 1 cm.

2. Structure characterization of polydopamine-coated SWCNT ($PS_{300}S_0$) and SWCNT (PS_0S_{50}) membranes.

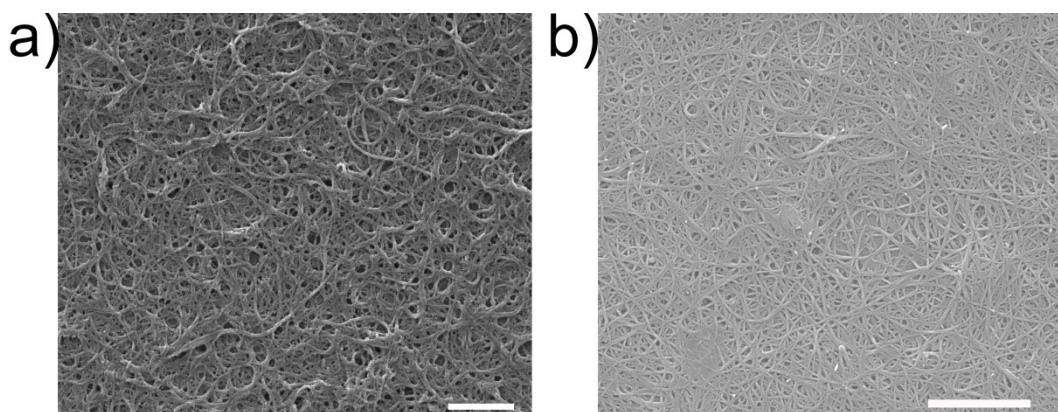


Figure S2. SEM images of polydopamine-coated SWCNT ($PS_{300}S_0$) and SWCNT (PS_0S_{50}) membranes. Scale bars = 1 μ m.

3. AFM images of bilayer membranes.

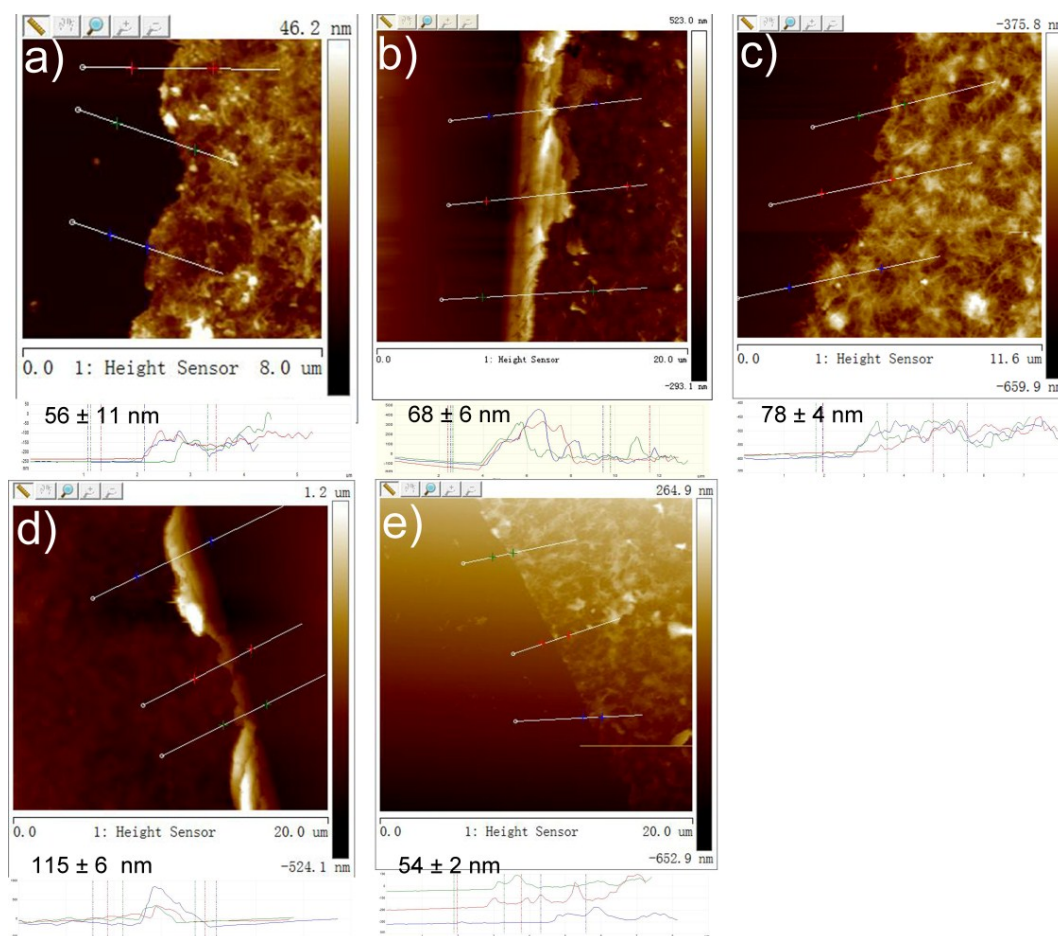


Figure S3. AFM cross-sectional images and analysis for (a) PS₃₀₀S₀, (b) PS₃₀₀S₁₀, (c) PS₃₀₀S₂₀ (d) PS₃₀₀S₅₀, (e) PS₀S₅₀ membranes. The surfaces were scratched with a razor to give SEM image contrast between the membrane and the Si substrate.

4. Apparatus for oil/water emulsions separation.

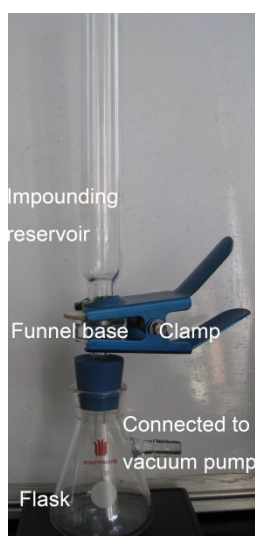


Figure S4. A digital photograph of pressure-driven oil/water emulsions separation apparatus.

5. Measurement of intrusion pressure.

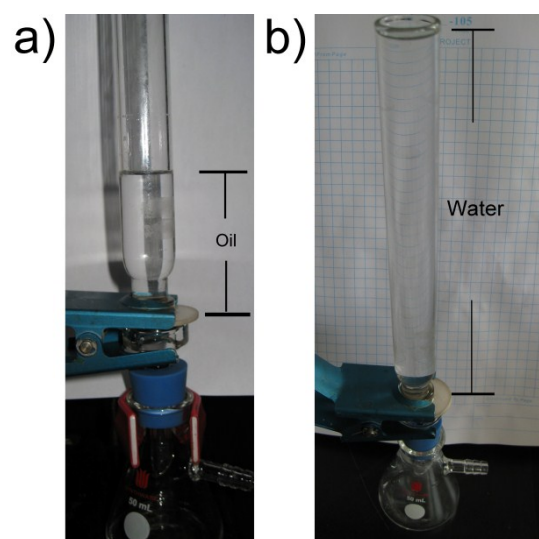


Figure S5. The measurements of intrusion pressure of (a) oil (chloroform as a symbol) and (b) water. As shown in Figure S5, a PS₃₀₀S₅₀ bilayer membrane can support 0.081 N of chloroform or 0.47 N of water without permeation. Effective filtration area is 0.785 cm². Therefore, the intrusion pressure of oil and water are ~ 0.01, ~ 0.06 bar, respectively.

6. Digital photographs and DLS data of water-in-cyclohexane and water-in-chloroform emulsions.

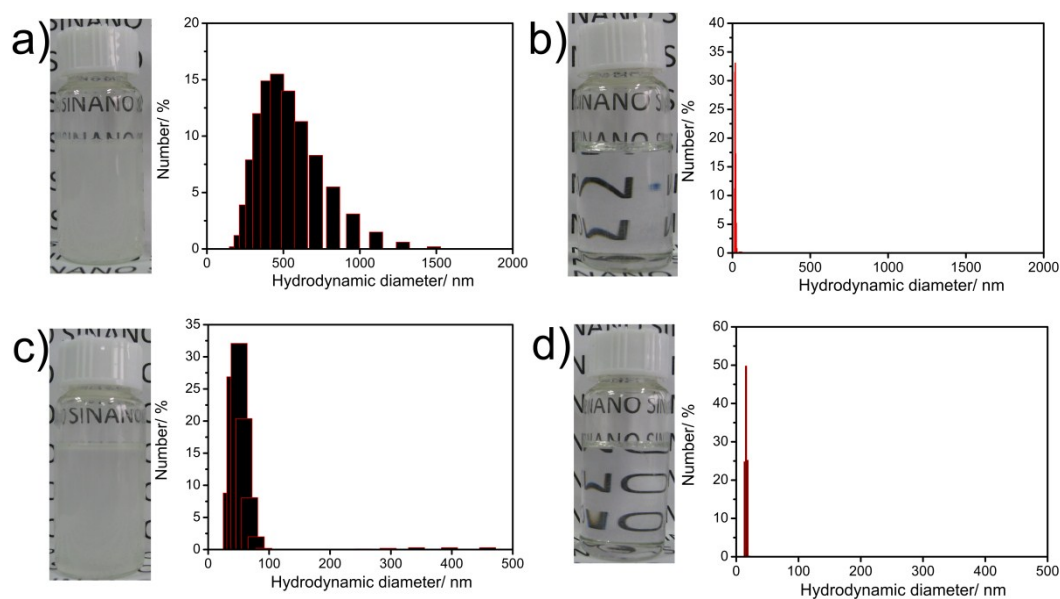


Figure S6. Digital photographs and DLS data of (upper) water-in-cyclohexane emulsion and (down) water-in-chloroform emulsion (a, c) before and (b, d) after filtration.

7. Variation of permeation flux as a function of SPAN 80 concentration in isooctane.

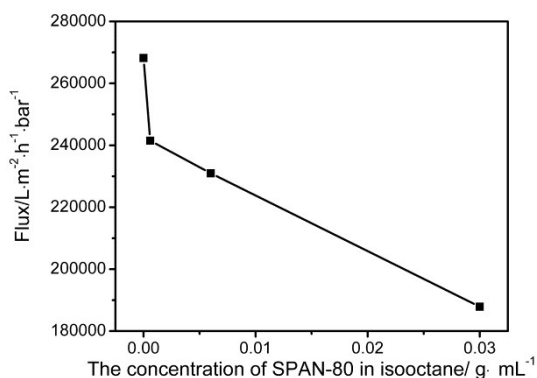


Figure S7. The variation of permeation flux as a function of SPAN 80 concentration in isooctane. A desired SPAN 80 was dissolved in isooctane without adding water. 5 mL of the solution was allowed to penetrate through a bilayer membrane. In this study, the concentration of SPAN 80 was in the range of 0.2 – 0.8 mg·mL⁻¹. As shown in Figure S7, J is decreased with increasing the concentration of SPAN-80 in isooctane. The concentration of SPAN 80 in this study is in range of 0.2 – 0.8 mg·mL⁻¹. And $J \approx 260000$ (0.2 mg·mL⁻¹), 235000 (0.8 mg·mL⁻¹), respectively. Therefore, 0.8 mg·mL⁻¹ of SPAN-80 may result in a decrease in J by $\sim 9.6\%$ so that we infer SPAN has much less influence in J .

8. Digital photographs and optical microscopy images of isooctane-in-water and *n*-hexane-in-water emulsions before and after filtration.

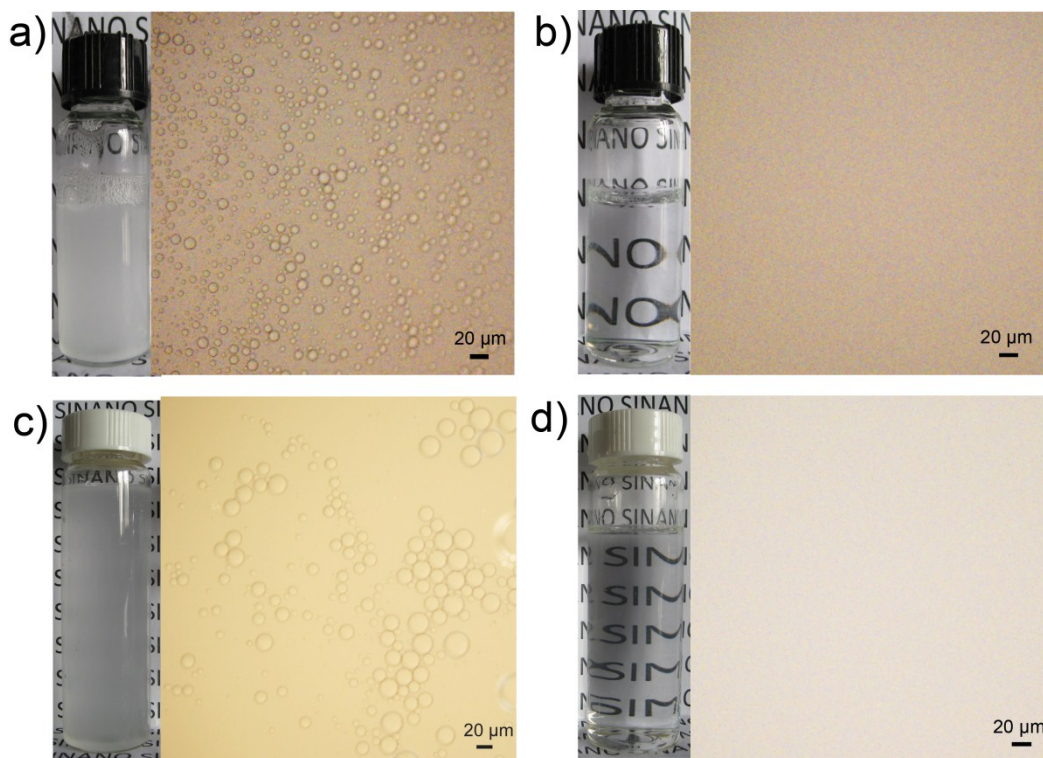


Figure S8. Digital photographs and optical microscopy images of (upper) isooctane-in-water emulsion and (down) *n*-hexane-in-water emulsion (a, c) before and (b, d) after filtration.

9. Analysis of forces acting on an oil droplet when permeating the bilayer membrane.

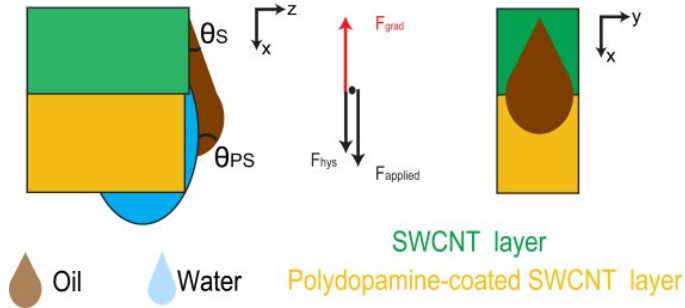


Figure S9. A schematic illustration regarding forces acting on an oil droplet. As shown in Figure S9, $F_{grad} = \gamma_{lg}(\cos\theta_s - \cos\theta_{ps})$ where γ_{lg} is the surface tension at oil–air interface, $\cos\theta_s$ and $\cos\theta_{ps}$ are the oil contact angles at the SWCNT surface and underwater polydopamine-coated SWCNT surface, respectively. Additionally, surface hysteresis provides an opposite energy barrier: $F_{hys} = \gamma_{lg} \int (\cos\theta_{ad,s} - \cos\theta_{re,ps}) dy$ where $\cos\theta_{ad,s}$ and $\cos\theta_{re,ps}$ are the advancing and receding contact angles at the SWCNT surface and underwater polydopamine-coated SWCNT surface, respectively, dy is the thickness of an oil droplet.

The total force applied on an oil droplet can be estimated:

$$F_{total} = F_{applied} - (F_{grad} - F_{hys})$$

We further define $F_{grad} - F_{hys} = F_{asy}$, therefore

$$F_{total} = F_{applied} - F_{asy}$$

Despite we acknowledged that F_{total} could be obtained quantitatively, but the results suggest that a desired F_{asy} could make oil droplet difficult penetrating the polydopamine-coated SWCNT layer.

10. Variation of permeation flux as a function of emulsifier concentration in water.

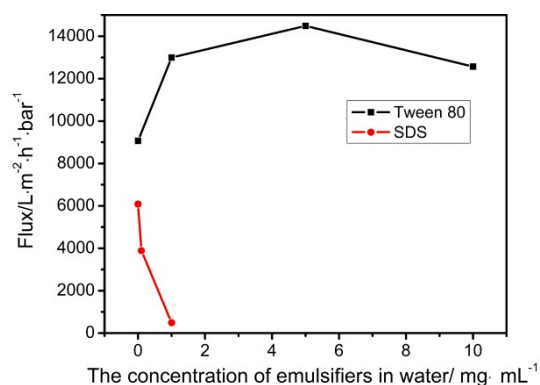


Figure S10. The variation of permeation flux as a function of emulsifier concentration in water. A desired tween 80 or SDS was dissolved in water without adding any oil. 5 mL of the solution was allowed to penetrate through a bilayer membrane. As shown in Figure S10, less amount of tween 80 reduces the surface tension of water, thus yielding a higher J . However, J is decreased when the concentration of tween 80 is raised above 6 mg·mL⁻¹. This reduced J might be caused by the membrane's fouling. Considering the amount of tween 80 used in this study, we found that 1 mg·mL⁻¹ of tween 80 may result in an increase in J by 43.3 %. And 10 mg·mL⁻¹ of Tween 80 yields an increase in J by 38.6 %. By contrast, SDS severely fouls the membrane, resulting in a sharp decrease in J by 35.6% (1 mg·mL⁻¹).

11.

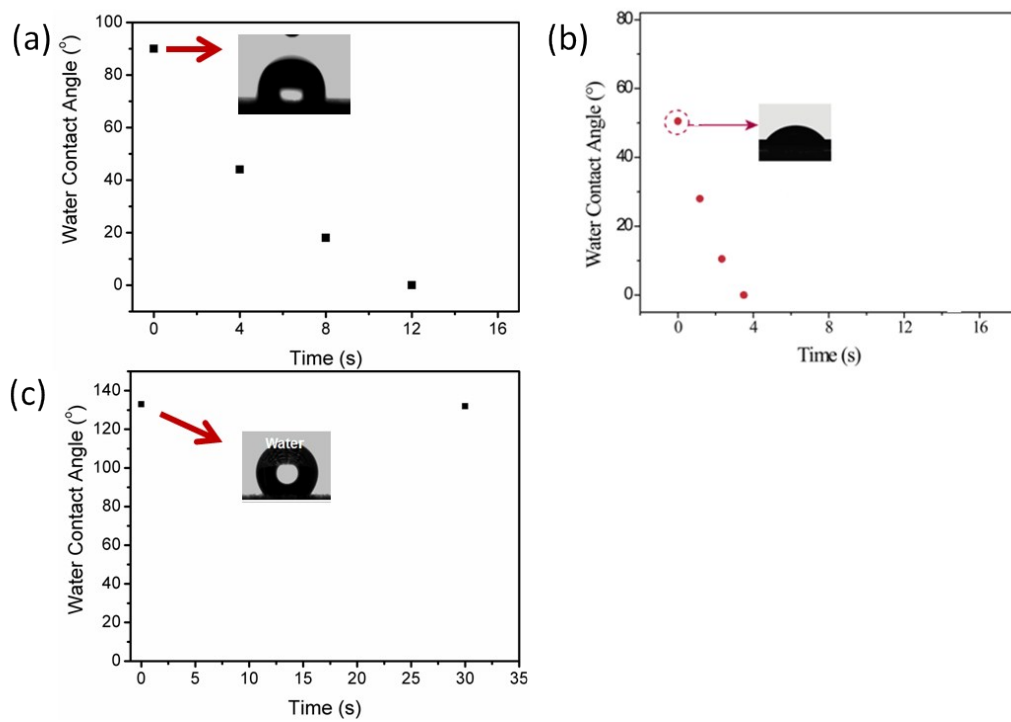


Figure S11. Surface wettability of (a) ceramic membrane, (b) MCE, and (c) copper mesh.

Table S1. Digital photographs of the filtrate for W/I and C/W emulsion passing through different membranes. The P applied is modulated according to the description in the manuscript.

Copper mesh + bilayer membrane: copper mesh supported bilayer membrane;
MCE + bilayer membrane: MCE membrane supported bilayer membrane.



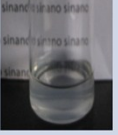




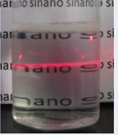



Emulsion	Copper mesh + bilayer membrane	MCE + Bilayer membrane	Ceramic membrane	MCE	Copper mesh
W/I					
C/W					

Table S2. Digital photographs of the filtrate for W/I and C/W emulsion passing through different membranes.

Hydrophilic ceramic membrane + hydrophobic SWCNT	Hydrophobic copper mesh + hydrophilic PD@SWCNT
C/W 	W/I 